DETECTION AND MAPPING OF OIL SLICKS IN THE SEA BY COMBINED USE OF HYPERSPECTRAL IMAGERY AND LASER-INDUCED FLUORESCENCE

Marc Lennon[1,2], Sergey Babichenko[3], Nicolas Thomas[1], Vincent Mariette[1], Grégoire Mercier[2] and Aleksei Lisin[3]

1. SAS ActiMar, 24 quai de la Douane, 29200 Brest, France; marc.lennon(at)actimar.fr
2. GET/ENST-Bretagne, CNRS UMR 2872 TAMCIC, Technopôle Brest-Iroise, CS 83818, 29238 Brest Cedex, France; gregoire.mercier(at)enst-bretagne.fr
3. AS Laser Diagnostic Instruments, 113A Kadaka Str., 12915 Tallinn, Estonia; sergeyb(at)ldi.ee

ABSTRACT

The demand for efficient detection, mapping and volume estimation of oil pollution in the sea is growing. Reliable observation tools are required to support monitoring flights against sea pollutions and to provide guidance for maritime and airborne means of fighting such occurrences. The present pilot project aimed at the evaluation of the combined use of airborne passive Hyperspectral Imagery (HI) and Laser Induced Fluorescence (LIF) technologies for remote sensing of oil spills in the sea.

The passive hyperspectral imager (CASI-2) and the Fluorescent Lidar System (FLS-AU) have been installed onboard a fixed-wing aircraft (Cessna 404). Test flights have been carried out over controlled simulated oil pollution at sea off the coast of Brittany, France, in May 2004. CASI data allowed very high spatial resolution (1 and 2 metres) slick maps to be produced, and the polluted surface to be estimated. LIF spectra acquired by FLS-AU allowed oil slick thickness to be locally estimated with approximate spatial resolution of 25 metres along the flight track. The data fusion procedure proved to be consistent with the radiative transfer model over a polluted water area including a thin layer of oil, and allowed a high resolution (1 metre) thickness map to be computed.

As a result of the studies the location, extents, and volume of the oil spilled were estimated from the maps. A critical study of the methodology used and a discussion on the precision reached by the quantitative estimates is proposed. The ways towards the design of an operational system including both passive and active airborne optical sensors for supporting recovering operations are discussed.

Keywords: hyperspectral, laser-induced fluorescence, oil spill survey.

INTRODUCTION

In May 2004, three real oil spills at sea were performed during a three-day campaign off the coasts of Britanny, France. The campaign, named DEPOL04, was carried out under the responsibility of the French Navy represented by the CEPPOL (Commission d'Etudes Pratiques sur les Pollutions) and of the French Customs, and managed by the CEDRE (Centre de documentation de recherche et d'expérimentations sur les pollutions accidentelles des eaux). The potentials of airborne passive hyperspectral imagery (1,2) and active fluorescence laser systems (3,4,5,6,7,8) for remote sensing of oil spills were studied separately in the past.

This controlled oil pollution offered the opportunity to test the joint operation of a hyperspectral imager (CASI-2) and a fluorescence lidar (FLS-AU) (9) for oil slicks detection and quantitative mapping. The pilot project was conducted by ActiMar, a French SME specialized in operational oceanography and high resolution remote sensing, in collaboration with GET/ENST-Bretagne (TIME team, CNRS UMR 2872 TAMCIC) and Laser Diagnostic Instruments (Tallinn) and was funded by the RITMER programme of the French Ministry of Research under the name

DETECSUIV. Radar satellites as well as airborne reconnaissance missions were used to obtain oil slicks localisation (10). Flight lines were prepared and integrated into a flight assistance system. CASI-2 and FLS-AU were installed onboard a fixed-wing aircraft (Cessna 404). Using an optimal flight configuration, 10 to 40 km² per hour could be recorded. In order to extract the useful parameters from CASI-2 and FLS-AU data, a specific processing chain was developed. CASI data allow high spatial resolution (1 and 2 metres) slicks maps to be produced, and the polluted surface to be estimated, after illumination corrections and definition of specific colour spaces taking advantage of observed spectral phenomena. Remote data acquisition has been supported by ground spectroscopic measurements of the slicks onboard a small boat. A simple optical model of light scattering in the water column was shown to be relevant for understanding the intra-slick spectral variability.

In-lab calibration of fluorescence spectra acquired by FLS with optical absorption of oil samples allowed the oil film thickness to be locally estimated. LIF data were used to "calibrate" the CASI data and to extend the estimation of thickness over all the CASI pixels. That data fusion procedure was shown to be consistent with the optical model over a polluted water area including a thin layer of oil, and allowed computation of very high spatial resolution (1 metre) thickness distribution maps. The maps were used to estimate the volume of the spilled oil. In order to show all the data processing steps, a demonstrator has been developed, starting from raw CASI-2 and FLS-AU data integration and fusion up to the visualisation of high spatial resolution oil thickness maps and oil pollution quantitative results.

The whole operational aspects of the campaign are described in (11), the principle of sensor operation and data processing chains are described in (12). This paper is more focused on the consideration of combined operational use of two sensors. The potentials and the limits of the whole approach are discussed and recommendations are made for the combined use of passive and active hyperspectral sensors as a reliable observation mean for supporting operational recovering operations at sea.

DATA ACQUISITION AND PROCESSING

The joint use of two sensors implies to consider the limitations of both. For a single CASI data acquisition, the flight altitude should be maximised in order to reach the maximum swath if the meteorological conditions are adequate. In the present case, the flight altitude was limited by the maximal possible flight altitude of the FLS-AU, which is 500 m (approx. 1500 ft). The speed of the acquisition should be minimised in order to acquire the maximum amount of data. The minimum speed, however, is limited by the capabilities of the platform. Using a Cessna 404, it is fixed at 100 kn to avoid turbulences. The compromised operational specs were used to provide data gathered by both sensors. Figure1 shows the operational schematics for two sensors.

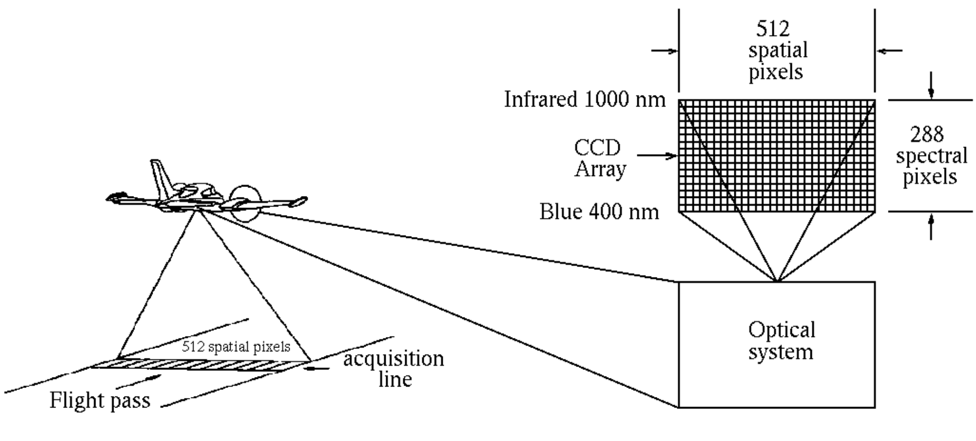

Figure 1a: Schematics of the CASI operation.

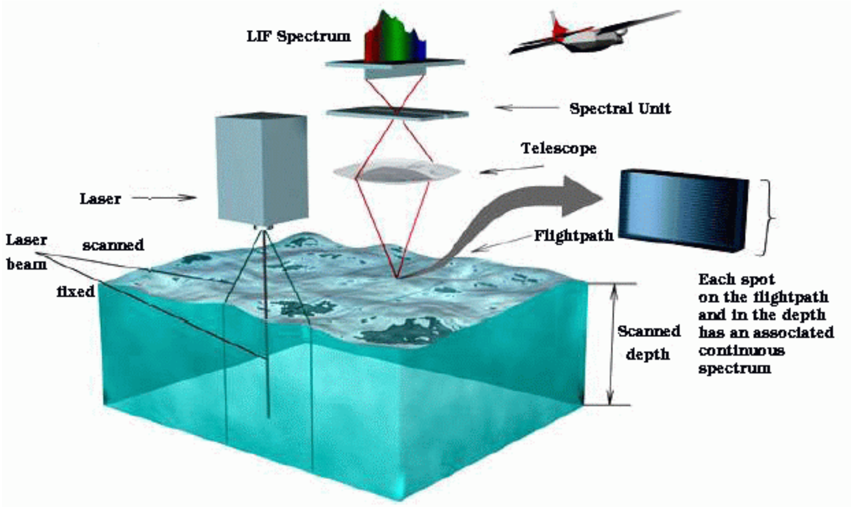

Figure 1b: Schematics of the FLS-lidar operation.

CASI

Considering the above-mentioned flight parameters, the CASI-2 was configured to operate with 18 equally distributed spectral channels over the spectral range of 400-1000 nm at a spectral resolution of 30 nm. The swath on the sea surface had a width of 380 m and spatial resolution of 1 m. Raw CASI data were calibrated into radiance units, geometrically corrected and geo-referenced by INS/dGPS data. Across-track illumination corrections were performed, and a mosaic of flight lines was built. Figure 2 shows examples of CASI spectra recorded over clear water, thin and thick oil films, during the DEPOL04 experiment.

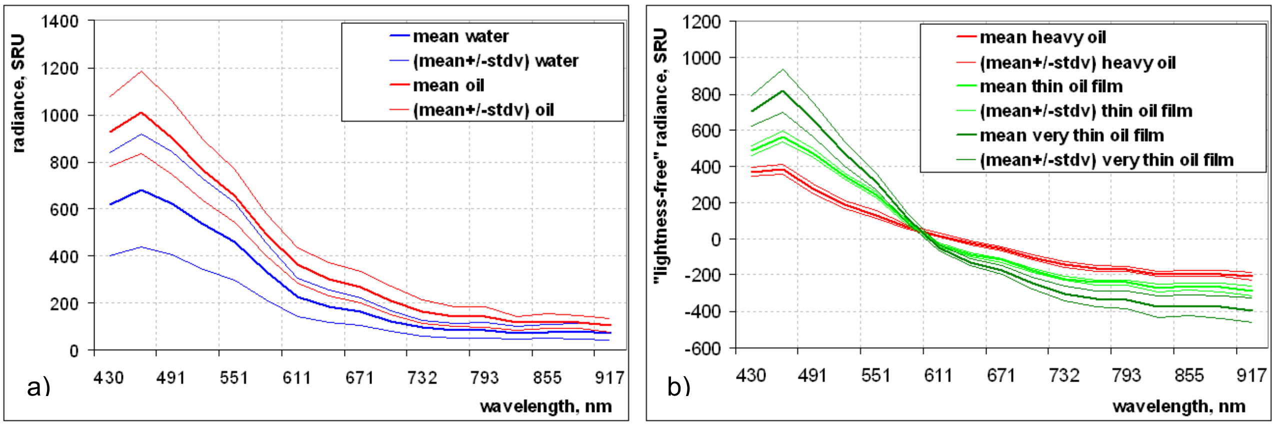

Figure 2: (a) Radiances L(λ) *as observed by CASI from clear water and oil polluted surfaces; (b) "Spectral rotation" as observed on "lightness-free" CASI spectra from different oil films.*

The DEPOL04 experiment has shown that the global radiation reflected by an oil polluted surface is higher than the radiation reflected by surrounding clear water because of higher specular reflection on the oil film surface (Figure 2a). The computation of "lightness-free" radiance $S(\lambda)$ was used to take into account the intra-slick intrinsic spectral variability. CASI experiments over the slicks spilled from the PRESTIGE tanker in 2002, as well as the current DEPOL04 experiment demonstrated that the spectral behaviour of $S(\lambda)$ depends on the oil film thickness: when the oil layer becomes thicker, the radiance decreases in the blue and increases in the near infrared part of the electromagnetic spectrum, leading to the so-called "spectral rotation" around 600 nm as a function of oil thickness (Figure 2b).

A 3-parameter model called "ALS" has been developed for CASI data processing (12). First, a standard three-layer optical model including air, a thin layer of oil, and water is used to relate the reflectance above the water surface to the thickness of the oil layer. This optical model, completed by spectroscopic measurements of direct solar radiance on the slick measured onboard the boat, is used in conjunction for the simulation of the signal reaching the sensor as a function of the thickness of the oil layer, in the whole spectral range of CASI-2 data. A procedure for the inversion of the model is built in order to compute, from the CASI-2 data, a parameter called *A* which is proportional to the oil thickness. The linear coefficient relating *A* to the thickness is a function of the diffractive index of water and oil and therefore remains unknown. In order to take also into account the specular reflexion on the slick surface, as well as the "saturation variability" induced by the thickness varibility over the slick, two other parameters, called *L* (global reflected radiation or "lightness") and *S* ("lightness-free radiance"), are computed as n-dimensional extensions of the "Lightness" and "Saturation" parameters used in the standard RGB to HLS colour transform. Those parameters allow the main information regarding oil and water to be reduced to three dimensions, which is very convenient to visually highlight the useful information into a "ALS" colour enhanced visualisation map. This so-called "ALS" 3-parameter model is also useful for the segmentation and data fusion processes. The full development of the processing chain can be found in (12).

FLS-AU lidar

The methods of oil spill detection with LIF technique are based on the depression of the water Raman line due to optical absorption in the oil film and the fluorescence of oil. The contrast method is used to estimate the oil film thickness by difference in Raman line intensity in clean and polluted water (3,7). The method of differential absorption is based on the distortion of the shape of Raman line due to dispersion of the water absorption coefficient (4) or comparison of Raman line intensities at different excitation wavelengths (5). A detailed analysis of these methods including fluorescence saturation spectroscopy is given in (8). Up to date most of the methods require additional information on optical properties of the spilled oil to provide absolute values of oil film thickness.

The FLS-AU lidar recorded LIF spectra of water and oil films in the spectral range of 300-500 nm at 308 nm excitation and a 20 Hz sampling rate. Rayleigh and Raman scattering, and fluorescence spectra are simultaneously read-out by a hyperspectral detector with 500 channels. The detector is operated in gated mode synchronised with the laser pulse: the gate pulse delay defines the sensing distance, and its duration of 0.5 µs eliminates the influence of ambient light to LIF spectra. The Raman line contrast method was used in the present studies. Recording the comprehensive LIF spectra provided a discrimination of clean and polluted waters, and oil fluorescence served as an indicator of the presence of oil (Figure 3).

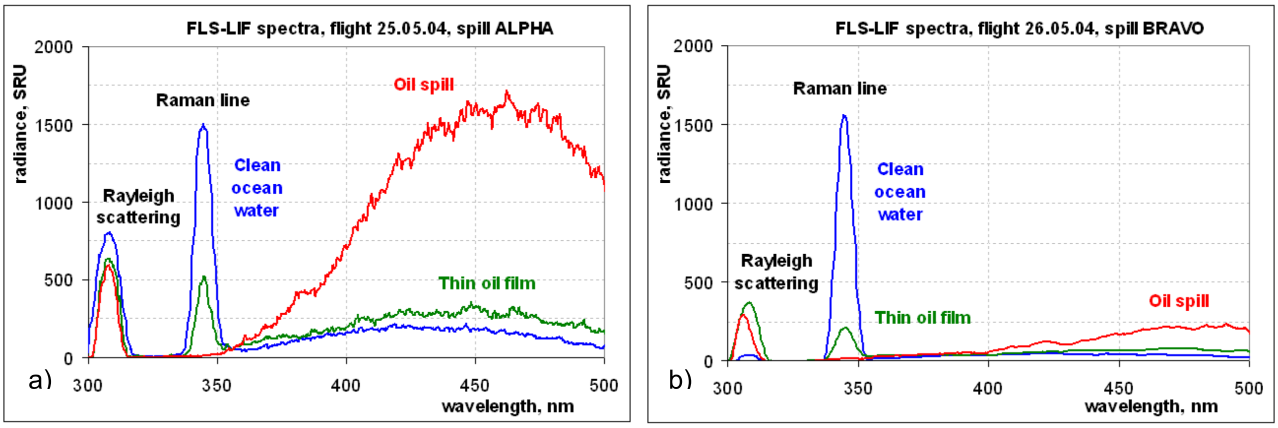

Figure 3: FLS-AU spectra recorded during the DEPOL04 experiment over water and oil films, (a) oil spill ALPHA, (b) oil spill BRAVO.

While the normal operational altitude range for FLS-AU is 50-300 m, in the present experiment it was used at 500 m altitude due to CASI operational requirements. This lowered the signal-to-noise ratio and required an accumulation of several LIF spectra to achieve good results. Therefore, the recorded lidar data have a lower spatial resolution on the ground (25 m along the flight track). Due to the down-looking optical layout of the FLS-AU lidar, the spatial resolution across the flight path was defined by the flight lines and constituted 200 m in average.

The raw FLS-AU spectra were geo-referenced with a handheld GPS receiver and accompanied with a time stamp allowing further LIF data alignment in accordance with INS/dGPS data. Examples of FLS-AU spectra recorded over clear water, and thin and thick oil films, during the DEPOL04 experiment are shown in Figure 3. It is noticeable that the Raman line intensity goes down when a thin oil film appears and disappears at a certain thickness, while the fluorescence intensity is increased with oil film thickness up to the saturation of fluorescence for a thick oil film.

The fluorescence exceeding the threshold corresponding to clean ocean water was considered as a primary indicator of oil detection, while the Raman line intensity served to quantify local oil film thicknesses. The attenuation coefficients of spilled oils were measured with a laboratory spectrophotometer after the experiment at the excitation (308 nm) and water Raman scattering (344 nm) wavelengths to convert the arbitrary thicknesses into absolute values.

Data fusion schematics

Figure 4 shows the whole processing chain for CASI + FLS-AU data fusion. Low frequency handheld GPS data jointly recorded with the FLS-AU dataset were temporally interpolated in order to correspond with high frequency/high accuracy data from the INS/dGPS data of the CASI dataset. In this way, high accuracy positioning data were associated to each thickness data. Re-sampling of the FLS-AU data over the same grid as CASI data led to accurate registration of both data sets.

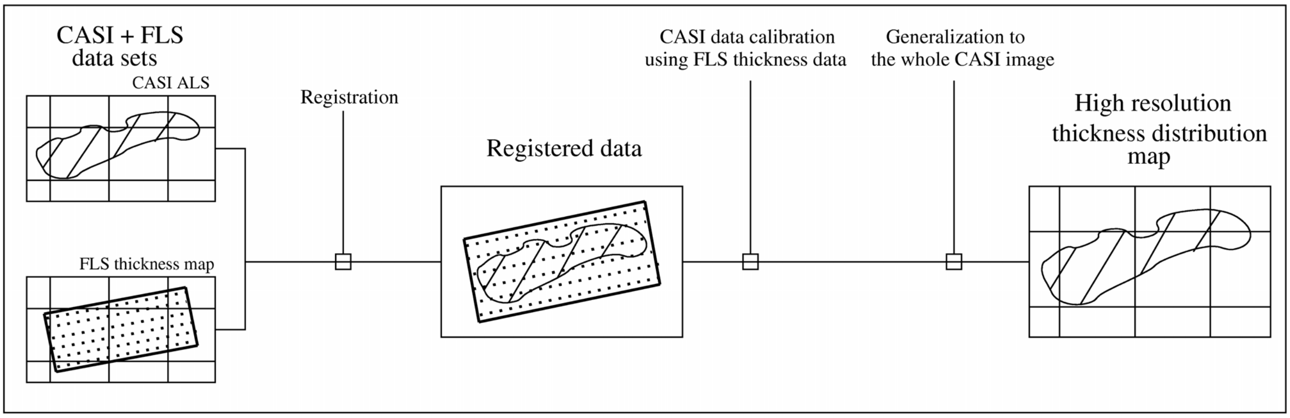

Figure 4: The CASI + FLS-AU data fusion chain.

According to the ALS decomposition model, the relative thickness parameter *A* extracted from the CASI dataset quasi-linearly depends on the thickness of the oil film on water in terms of the thin layer optical model. This parameter *A* can be calibrated by absolute thickness estimations obtained from the FLS-AU dataset. The calibration was done using the correlation between the *A* value and oil thickness measurements by lidar over the coinciding pixels in two data sets. The calibration was applied to all pixels of the CASI data set in order to get a high resolution thickness spatial distribution map. Illustration and results of the data fusion procedure can be found in (12). The surface and volume of the spills were estimated based on the integration of local pixel values over the whole slick image.

RESULTS

CASI and FLS data fusion

Three 10 m^3 oil slicks, Alpha, Bravo, and Charlie, were spilled during the DEPOL04 experiment. The Alpha slick was crude oil, while Bravo and Charlie included 65% HFO + 35% LCO. Figure 5 shows the spatial maps of the Alpha slick produced by CASI and interpolated with FLS lidar data. It is clearly noticeable that geographical location, size and shape of the slick image produced by the two sensors are quite similar. The width of the slick displayed by FLS-lidar is wider than by CASI. This is due to two reasons. First, the lidar detected oil film with thickness below 1 μm, and therefore the central part of the slick is encircled by a thin oil film. Second, the lidar map was created by data interpolation from several flight lines over the oil spill which were shifted in time, and in fact represents an averaged map of the spill movement on the water surface. The water Raman line disappeared in the central part of the slick (red zone in Figure 5b). The thickness estimation was only done by fluorescence intensity.

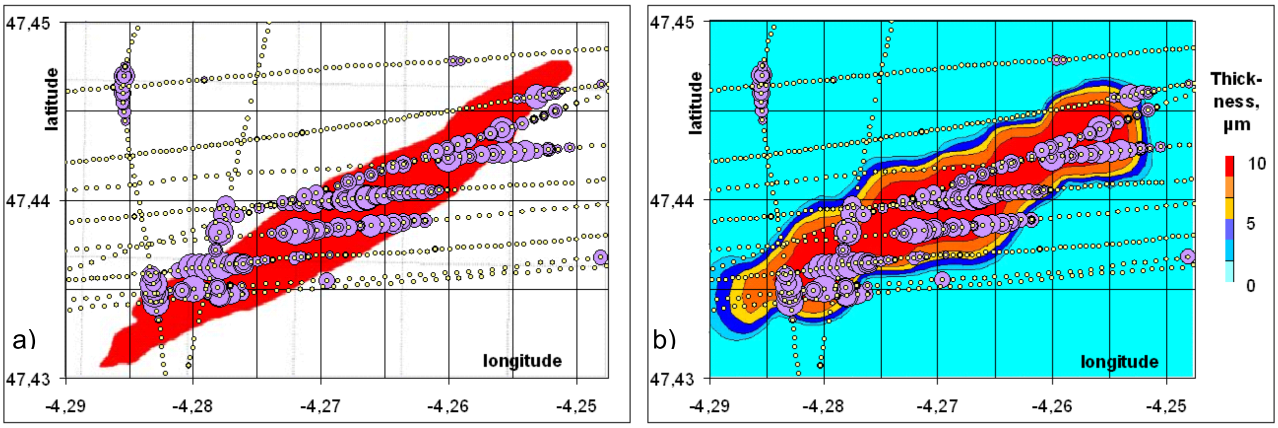

Figure 5: ALPHA oil spill, (a) slick map from CASI imagery, (b) FLS map. The size of the bubbles corresponds to the local thickness inside the spill, and the coloured contour plot reflects interpolated oil film thickness.

An example of a CASI enhanced colour visualisation map computed from the ALS decomposition of Charlie slick is shown in Figure 6. The map allows one to get a first qualitative assessment of the pollution. The distribution of the volume of the oil is highly revealed in the image (from blue to red) and shows that the maximum concentration of oil is located on the west side of the slick in a small area compared to its whole extent.

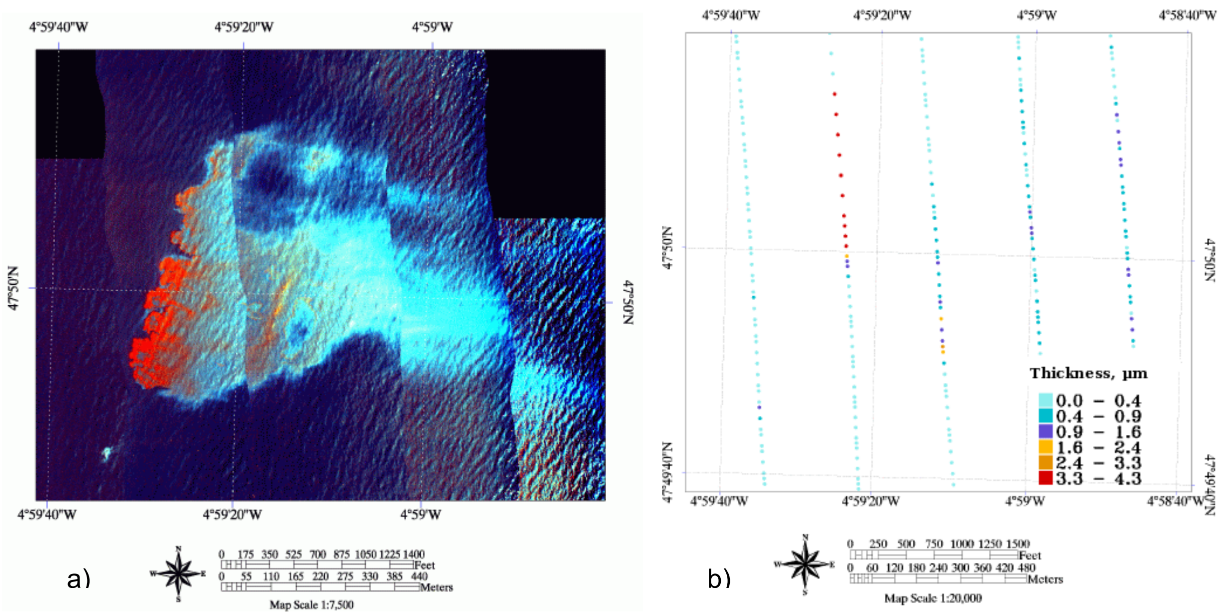

Figure 6: Slick Charlie. (a) "ALS" enhanced visualisation map, (b) local oil thickness measured by FLS-lidar.

The segmentation of the CASI ALS map allowed to derive the accurate localisation and geographical configuration of the slick. The exact extents of the slick can be computed. The CASI-2 and FLS-AU data fusion process leads to the computation of the high resolution thickness distribution map (Figure 7). The colours associated to the estimated thickness are quantitatively reported in the legend. This map confirms the qualitative assessment of the CASI enhanced visualisation map, and allows the whole volume of the spilled oil to be estimated.

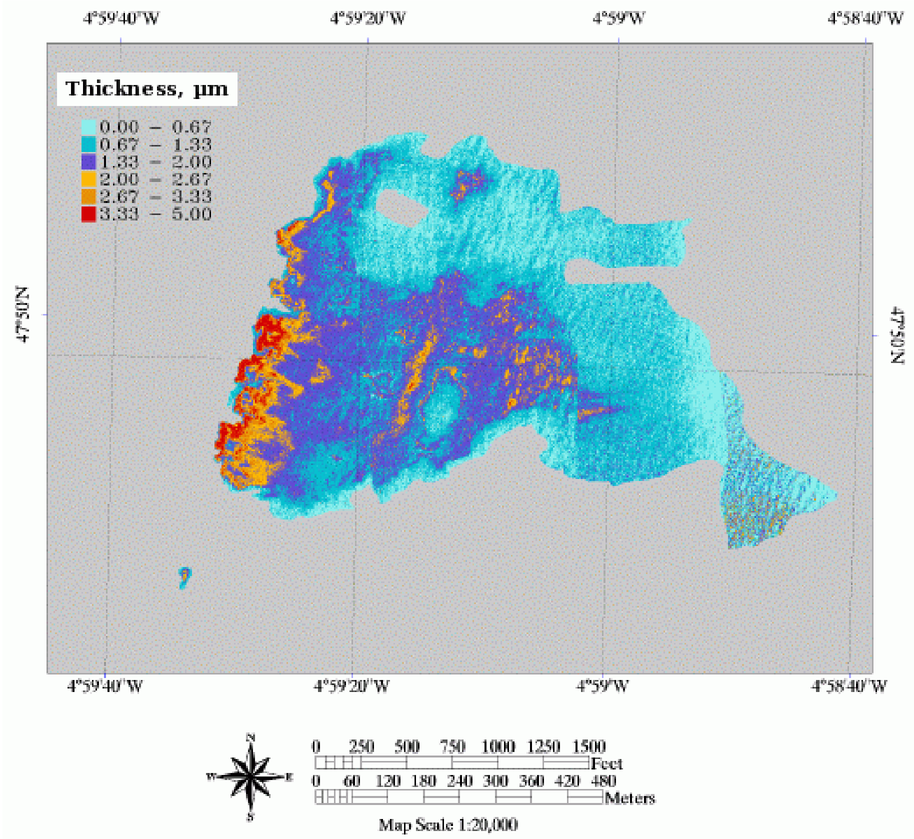

Figure 7: High resolution thickness distribution map of slick Charlie.

Discussion

The quantitative results are listed in Table 1. "Estimated surface" column represents the oil surface estimated over the polluted region estimated from the CASI images (Figure 7). "Volume by CASI" column represents the oil volume estimated over the high resolution thickness distribution map, calibrated by FLS-AU lidar data (Figure 7). "Volume by FLS" column represents the oil volume estimated by interpolation of FLS-data only (Figure 5b). The results show that the volumes have been underestimated for each slick. This is mainly due to the saturation of the optical measurements after a critical thickness was observed.

In the current experiment, the FLS-AU measurements were saturated at approximately 10 µm for Alpha, and 5 µm for Bravo and Charlie (i.e., the water Raman signal disappeared). Laboratory studies with all oil samples completed after the experiment showed that the Bravo and Charlie oils had 4 to 6 times lower fluorescence than the Alpha oil (compare "Oil spill" spectral curves in Figure 3), while their optical absorption in the UV range was 2 times higher. Therefore, a better estimation was achieved for slick Alpha.

Indeed, where the water Raman signal dropped to zero for the Alpha oil, the fluorescence intensities in the LIF spectrum allowed to estimate thick oil slick. At the same time, the fluorescence was already near the saturation at the thickness of approximately 20 µm in the central part of the slick. It resulted in an underestimation of the slick volume (2.08 m^3 and 5.1 m^3 based on FLS and CASI data, respectively, *versus* 10 m^3 of spilled oil). The higher volume derived with the lidar for the Alpha oil is due to two facts: first, the lidar registered also thin films around the central part of the slick detected by CASI (compare the shapes of the slick maps in Figure 5); and second, the number of laser points on the slick was a bit low to get a precise representation of the local thickness spatial distribution over the slick.

For the slicks Bravo and Charlie the fluorescence was hardly detectable due to lower fluorescence efficiency and strong optical absorption in the oil film. Mainly thin layers were accurately quantified with FLS and consequently the high resolution thickness distribution map was calibrated by lowered values. The experimental conditions with the slicks Bravo and Charlie were very unfavourable, both for LIF measurements and the CASI data calibration.

The estimated thicknesses were quite accurate over thin layers, therefore the most dispersed the volume is over a large surface, the most accurate the estimation of the volume could be. In the current experiment, the slicks were not dispersed as much since the data acquisition was performed a few hours after the spill. Hence, the system capabilities were limited to provide the minimal bound of the real volume of oil spilled, which should, however, be considered as reliable.

The high resolution thickness distribution maps allow, despite the saturation areas, the limits of the slick and the spatial distribution of volumes to be reliably represented. This information is *a priori* the most important for the support of operational aerial and/or maritime recovering operations.

Table 1: Quantitative results.

Slick	Estimated surface (km^2)	Volume by CASI (m^3)	Volume by FLS-AU (m^3)
Alpha	0.97	2.08	5.1
Bravo	0.34	0.36	0.38
Charlie	0.39	0.49	0.26

CONCLUSIONS

The data fusion from both sensors allows a spatial distribution of oil film thickness to be geographically mapped with high resolution. A demonstrator including the data processing chain has been developed as a basis for future operational software development. The combined use of two sensors mitigates the limitations of each one operated separately. The lidar is more accurate in estimations of thin oil films and can provide local quantitative data for CASI images. Hyperspectral imaging delivers clear geographical references for oil slicks assisting to distinguish clean and polluted water in LIF analysis.

The scanning features of FLS-lidar will definitely improve the accuracy of mapping, and therefore the precision of high resolution CASI data. A lidar operation at several excitation wavelengths will allow to map the oils with higher aliphatic content using differential absorption at bi-harmonic operation. These features are already realised in the new FLS-AM model of Laser Diagnostic Instruments.

The parameterisation of the radiative transfer model for oil slicks floating on the ocean still needs improvements. In particular, the thin layer optical model is used without any approximations in conjunction with atmospheric parameters and water leaving radiance estimations in order to estimate the signal reaching the sensor. Surface wave numerical models will be used to simulate a whole hyperspectral data cube, and a robust inversion procedure will be constructed. In the near future, the system will be tested onboard an airborne integrated platform, including data communication from the aircraft to the vessels in charge of recovering operations at sea, in order to support the operational fight and the guidance of the vessels.

This pilot project allowed us to make a step towards answering environmental concerns associated with accidents in oil storage and transportation. Passive and active hyperspectral sensors have been shown to be complementary. We think that the combined use of these sensors as a reliable observation means for supporting operational recovering operations is a high potential value-added application.

ACKNOWLEDGEMENTS

The authors would like to thank CEPPOL, Douanes Françaises and CEDRE for having supported and managed the DEPOL04 experiment, and for having accepted our participation. They also would like to thank the RITMER committee from the French Ministry of Research for the financial co-funding of the project, as well as the European Union for co-funding the remote sensing activities at ActiMar through the FEDER (Fonds Européens de Développement Régional) fundings.

REFERENCES

1 Byfield V, 1998. Optical remote sensing of oil in the marine environment. PhD Thesis (University of Southampton, UK)

2 Lennon M, V Mariette, A Coat, V Verbeque, P Mouge, GA Borstad, P Willis, R Kerr & M Alvarez, 2003. Detection and mapping of the November 2002 PRESTIGE Tanker oil spill in Galicia, Spain, with the airborne multispectral CASI sensor. In: 3rd EARSeL Workshop on Imaging Spectroscopy ,13-16 may 2003, Oberpfaffenhofen, Germany, edited by M Habermeyer, A Müller & S Holzwarth (EARSeL, Paris) 245-251

3 Reuter R, H Wang, R Willkomm, K Loquay, T Hengstermann & A Braun, 1995. A laser fluorosensor for maritime surveillance: Experimental results. EARSeL Advances in Remote Sensing, 3(3): 152-169

4 Patsayeva S, V Yuzhakov, V Varlamov, R Barbini, R Fantoni, C Frassanito & A Palucci, 2000. Laser spectroscopy of mineral oils on the water surface. EARSeL eProceedings, 1(1): 106-114

5 Chubarov V V, T A Deydan, V V Fadeev & P S Petrov, 1995. New remote method for measurement of oil slick thickness on water surface. In: 3rd Thematic Conference on Remote Sensing for Marine and Coastal Environments, (Seattle, Washington, USA) 1: 433-440

6 Babichenko S, A Dudelzak & L Poryvkina, 2002. Laser sensing technologies in studies of marine and coastal environment. In: The Seventh International Conference on Remote Sensing for Marine and Coastal Environments, Miami, Florida, 20-22 May 2002, eProceedings, Veridan, 8 pp. (vailable on CD ROM)

7 Brown C E & M F Fingas, 2003. Review of the development of laser fluorosensors for oil spill application. Marine Pollution Bulletin, 47: 477-484

8 Chubarov V V, V V Fadeev, S M Glushkov & V A Shaporev, 1997. Remote laser diagnostics of oil films on water surface using fluorescence saturation spectroscopy. In: 3rd EARSeL Workshop on lidar remote sensing of land and sea, edited by S Babichenko & R Reuter (EARSeL, Paris) 163-168

9 Babichenko S, A Dudelzak & L Poryvkina, 2004. Laser remote sensing of coastal and terrestrial pollution by FLS-Lidar. EARSeL eProceedings, 3(1): 1-8

10 Lennon M, S Babichenko, N Thomas, V Mariette & G Mercier, 2005. Oil slick detection and characterization by satellite and airborne sensors: experimental results with SAR, Hyperspectral and Lidar data. In: IEEE IGARSS' 2005, Seoul, Korea, 25-29 July 2005 (available on CD ROM)

11 Lennon M, N Thomas, V Mariette, S Babichenko & G Mercier, 2005. Operational quantitative mapping of oil pollutions at sea by joint use of an Hyperspectral Imager and a Fluorescence Lidar System on-board a fixed-wing aircraft. In: IEEE OCEANS' 2005, Brest, France, 20-23 June 2005 (available on CD ROM)

12 Lennon M, S Babichenko, N Thomas, V Mariette, & G Mercier, 2005. Combining passive hyperspectral imagery and active fluorescence laser spectroscopy for airborne quantitative mapping. In: 4th EARSEL Workshop on Imaging Spectroscopy, Warsaw, Poland, 27-29 April 2005 (EARSeL, Strasbourg)